Nonequilibrium model of ultrafast laser-induced electron photofield emission from a dc-biased metallic surface

L. Wu and L. K. Ang*
School of Electrical and Electronic Engineering, Nanyang Technological University, Singapore 639798, Singapore
(Received 10 October 2008; published 31 December 2008)

This paper proposes a nonequilibrium model to describe the ultrafast laser-excited electron photofield emission from a metallic surface with an applied dc voltage. Using a microscopic kinetic approach based on Boltzmann's equation, we determine the nonequilibrium electron distribution due to the ultrafast laser excitation on metal and calculate the time dependence of the emitted electron charges and current density. Our calculation is able to explain the prior experimental observations without using the optical-field emission, which was disputed among the experiments. Inconsistency of the prior models used to explain the experimental results is discussed.

DOI: 10.1103/PhysRevB.78.224112 PACS number(s): 79.70.+q, 29.25.Bx, 85.45.Db

I. INTRODUCTION

Ultrafast electron microscopy, diffraction, and crystallography[1] are able to provide ultrafast time-resolved information of the underlying dynamics in physics, chemistry, and biology.[2–5] To probe the microscopic structural dynamics, a complete control over the spatiotemporal characteristics of the ultrafast electron pulse is required. A recent promising method is to use a low-power femtosecond laser to trigger sub-laser-duration free-electron pulses from a dc-biased metallic field emitter.[6–9] At higher charge (nC) and longer time (ps) scale, high brightness short electron bunches with low emittance have also been produced by the laser-photofield emission cathode[10] and rf photoinjectors,[11] which are critical for future light sources such as x-ray free-electron lasers.

Understanding the time-dependent emission process within the laser pulse is important to realize the sub-laser-duration electron pulse by using ultrafast laser-excited electron emission from sharp emitters with a dc applied voltage.[7–9] There have been some debates on the emission mechanism, such as optical-field emission,[7] multiphoton emission,[8] and multiphoton absorption followed by overbarrier emission.[9] For example, the optical-field emission reported[7] was not observed in a similar experiment.[9] Note that all the proposed models[7–9] have been restricted to equilibrium models, which may not be valid for emission at ultrashort time scale, and the laser-metal interaction was ignored completely.

These experiments[7–9] were conducted in the nonadiabatic tunneling regime with a Keldysh parameter of $1<\gamma<10$, which had also been studied intensively to understand the optical ionization of atoms and molecules.[12–14] The theory of ionization of atoms exposed to high-intensity laser radiation is based on the Keldysh model,[15] which indicates the regimes of optical-field tunneling ($\gamma \ll 1$) and multiphoton absorption ($\gamma \gg 1$). In comparison, it is relatively unclear in the theory at the nonadiabatic tunneling regime.[14] However, the Keldysh model cannot directly be used to describe the emission process in the ultrafast electron emission from sharp emitters as compared to ionization of atoms or molecules. First, the interaction among the electron, the lattice (phonon), and the laser electric field must be taken into account when a metal is exposed to laser radiation.[16,17] Second, there is a sufficiently large dc applied field that is comparable to the time-varying laser optical field, i.e., there always exists a dc field emission process besides the other two processes due to the laser optical field (multiphoton overbarrier emission and optical-field emission). In this paper, we will present a nonequilibrium model to account for the laser-metal excitation, which is able to explain the prior experimental findings[7–9] without using the disputed optical-field emission mechanism. The comparison with the simplified models[7] used before to explain the experimental results will be presented.

II. NONEQUILIBRIUM MODEL

Consider a laser pulse focused on the surface of a metallic target is absorbed by the electrons in the conduction band, leaving the lattice unperturbed due to its heat capacity, which generates a nonequilibrium condition. The transition to equilibrium state is governed by electron-electron (e-e) and electron-phonon (e-p) collisions, which occurs, respectively, at <100 fs (internal thermalization) and from 100 fs to up to a few picoseconds (external thermalization). For a picosecond laser, the electron gas quickly achieves the internal thermalization through the e-e collisions, but the electron-lattice system is still far from equilibrium at the end of laser pulse. At this condition, the classical two-temperature model (TTM) is normally used by assigning two different temperatures for electron (T_e) and phonons (T_i), whose energy exchange is governed by the electron-phonon collisions. One good example of TTM is the time-dependent field-assisted photoemission model proposed by Jensen *et al.*,[18] which have been used to explain picosecond laser-excited ZrC field emission.[10]

For a femtosecond laser, the e-e collisions are however not fast enough to reach the internal thermalization during the laser pulse. Thus the TTM is inadequate and microscopic kinetic approach should be used, such as Boltzmann's equation[16,17] and nonequilibrium Green's-function theory.[19] The femtosecond laser excitation of the metallic tip will generate a nonequilibrium electron distribution $f(E,t)$ with a pronounced population above the Fermi energy E_F, and the

electrons are emitted from the surface. For simplicity, our model is based on Boltzmann's equation of a simplified metal description with a parabolic and isotropic conduction band, and the phonon-dispersion relation is described by the Debye model. The temporal profile of the laser pulse is assumed to be a step function from $t=0$ to τ in all calculations, and the spatial variation in pulse intensity is neglected.

To investigate the nonequilibrium dynamics of electrons in metals irradiated with a laser pulse of moderate intensity, we follow Rethfeld's approach[16] to use a time- and energy-dependent kinetic description, applying Boltzmann's collision integrals explicitly without using any relaxation-time approximation. The photon energy absorption, *e-e* interaction, and *e-p* interaction are included in a system of Boltzmann's equations to obtain the temporal evolution of the distribution function of the electron gas $f(k)$ and the phonon gas $g(q)$,

$$\frac{\partial f(k)}{\partial t} = \left.\frac{\partial f(k)}{\partial t}\right|_{e\text{-}e} + \left.\frac{\partial f(k)}{\partial t}\right|_{e\text{-}p} + \left.\frac{\partial f(k)}{\partial t}\right|_{\text{absorb}},$$

$$\frac{\partial g(q)}{\partial t} = \left.\frac{\partial g(q)}{\partial t}\right|_{p\text{-}e}. \tag{1}$$

Here, $f(k)$ and $g(q)$ depend on the modulus of the momentum $\boldsymbol{k}$ and $\boldsymbol{q}$. Before laser irradiation, $f_0(k)$ and $g_0(q)$, respectively, are assumed to be Fermi-Dirac and Bose-Einstein distributions at room temperature. The phonon gas is affected only by the electron gas, the energy absorption by the lattice directly from the laser, and the phonon-phonon collisions are neglected.

A. Electron-electron collisions

Electron-electron collisions lead to energy relaxation within the electron gas through which the absorbed photon energy is distributed among the free electrons so that the electron gas tends toward a thermal equilibrium (a Fermi distribution). From the first-order perturbation-theory framework, the collision term that describes the *e-e* interaction, i.e., the sum over all possible two-body scattering events in three dimensions which populate and depopulate the state $\boldsymbol{k}$ is given by[16,17]

$$\left.\frac{\partial f(k)}{\partial t}\right|_{e\text{-}e} = \frac{2\pi}{\hbar}\sum_{\boldsymbol{k}_1,\boldsymbol{k}_2,\boldsymbol{k}_3} |M_{ee}|^2 F(\boldsymbol{k},\boldsymbol{k}_1,\boldsymbol{k}_2,\boldsymbol{k}_3) \times \delta(\boldsymbol{k}+\boldsymbol{k}_1-\boldsymbol{k}_2-\boldsymbol{k}_3) \times \delta[E(k)+E(k_1)-E(k_2)-E(k_3)], \tag{2}$$

with $F(\boldsymbol{k},\boldsymbol{k}_1,\boldsymbol{k}_2,\boldsymbol{k}_3) = -f(\boldsymbol{k})f(\boldsymbol{k}_1)[1-f(\boldsymbol{k}_2)][1-f(\boldsymbol{k}_3)] + f(\boldsymbol{k}_2)f(\boldsymbol{k}_3)[1-f(\boldsymbol{k})][1-f(\boldsymbol{k}_1)]$. The momentum and energy conservation conditions appear, and the Pauli exclusion principle, $f(\boldsymbol{k})f(\boldsymbol{k}_1)[1-f(\boldsymbol{k}_2)][1-f(\boldsymbol{k}_3)]$, takes into account the probability that the $\boldsymbol{k}$ and $\boldsymbol{k}_1$ states are occupied while the $\boldsymbol{k}_2$ and $\boldsymbol{k}_3$ states are empty. The interaction matrix element M_{ee} is derived from a screened Coulomb potential, and it depends on the scattering transferred momentum $\Delta\boldsymbol{k}=\boldsymbol{k}_1-\boldsymbol{k}_2=\boldsymbol{k}_3-\boldsymbol{k}$ and the static screening length κ_{sc},[16]

$$|M_{ee}|^2 = \left[\frac{e^2}{\epsilon_0 V}\frac{1}{\Delta k^2+\kappa_{\text{sc}}^2}\right]^2,$$

where

$$\kappa_{\text{sc}}^2 = \frac{e^2 m_e}{\pi^2\hbar^2\epsilon_0}\int_0^\infty f(k)dk. \tag{3}$$

Here, the screening length κ_{sc} represents an important parameter for the electron-electron interaction and is calculated at each time step for the updated distribution function $f(k)$, while m_e is the effective mass of a free electron in the conduction band.

B. Electron-phonon collisions

Electron-phonon collisions transfer energy from the laser-heated electron gas to cold lattice. The electron-phonon interaction consists in phonon emission and absorption process by the electron gas. The phonon emission and absorption scattering rates can be calculated through Fermi's golden rule in the framework of the first-order perturbation theory. Therefore the electron distribution change in the state $\boldsymbol{k}$ due to the *e-p* collisions is given by the sum of two terms, representing the total scattering rate of both phonon emission and absorption processes, involving transition toward all the states, $\boldsymbol{k}^+=\boldsymbol{k}+\boldsymbol{q}$ and $\boldsymbol{k}^-=\boldsymbol{k}-\boldsymbol{q}$. The collision terms for the electron-phonon interaction read as[16,17]

$$\left.\frac{\partial f(k)}{\partial t}\right|_{e\text{-}p} = \frac{2\pi}{\hbar}\sum_{\boldsymbol{q}} |M_{ep}|^2 \{S^-(\boldsymbol{k},\boldsymbol{q}) \times \delta[E(k)-E(k^-) - E_{\text{ph}}(q)] + S^+(\boldsymbol{k},\boldsymbol{q}) \times \delta[E(k)-E(k^+) + E_{\text{ph}}(q)]\}, \tag{4}$$

$$\left.\frac{\partial g(q)}{\partial t}\right|_{p\text{-}e} = 2\times\frac{2\pi}{\hbar}|M_{ep}|^2\sum_{\boldsymbol{k}} S^+(\boldsymbol{k},\boldsymbol{q}) \times \delta[E(k)-E(k^+) + E_{\text{ph}}(q)], \tag{5}$$

where $S^-(\boldsymbol{k},\boldsymbol{q}) = f(\boldsymbol{k}^-)[1-f(\boldsymbol{k})]g(\boldsymbol{q}) - f(\boldsymbol{k})[1-f(\boldsymbol{k}^-)][1+g(\boldsymbol{q})]$ and $S^+(\boldsymbol{k},\boldsymbol{q}) = f(\boldsymbol{k}^+)[1-f(\boldsymbol{k})][1+g(\boldsymbol{q})] - f(\boldsymbol{k})[1-f(\boldsymbol{k}^+)]g(\boldsymbol{q})$. For example, an electron in state $\boldsymbol{k}$ can scatter into state $\boldsymbol{k}^-$ by emitting a phonon with wave number $\boldsymbol{q}$, the factor $f(\boldsymbol{k})[1-f(\boldsymbol{k}^-)][1+g(\boldsymbol{q})]$ takes into account the Pauli exclusion principle, as electron can scatter only into unoccupied states $[1-f(\boldsymbol{k}^-)]$. The proportionality of the phonon emission processes on the factor $[1+g(\boldsymbol{q})]$ is due to both the spontaneous and stimulated emission. On the other hand, the phonon absorption probability (e.g., an electron in state $\boldsymbol{k}^-$ scattering into state $\boldsymbol{k}$) should be proportional to $g(\boldsymbol{q})$ instead of $[1+g(\boldsymbol{q})]$. The term $\delta[E(k)-E(k^-)-E_{\text{ph}}(q)]$ represents the total-energy conservation condition. The *e-p* matrix element is[17]

$$|M_{ep}|^2 = \frac{1}{2\epsilon_0 V}\frac{e^2}{q^2+\kappa_{\text{sc}}^2}E_{\text{ph}}(q), \tag{6}$$

where $E_{\text{ph}}(q)=\hbar v_s q$ is the energy of a phonon with the modulus of wave vector q and v_s is the sound speed of longitudinal phonon.[16]

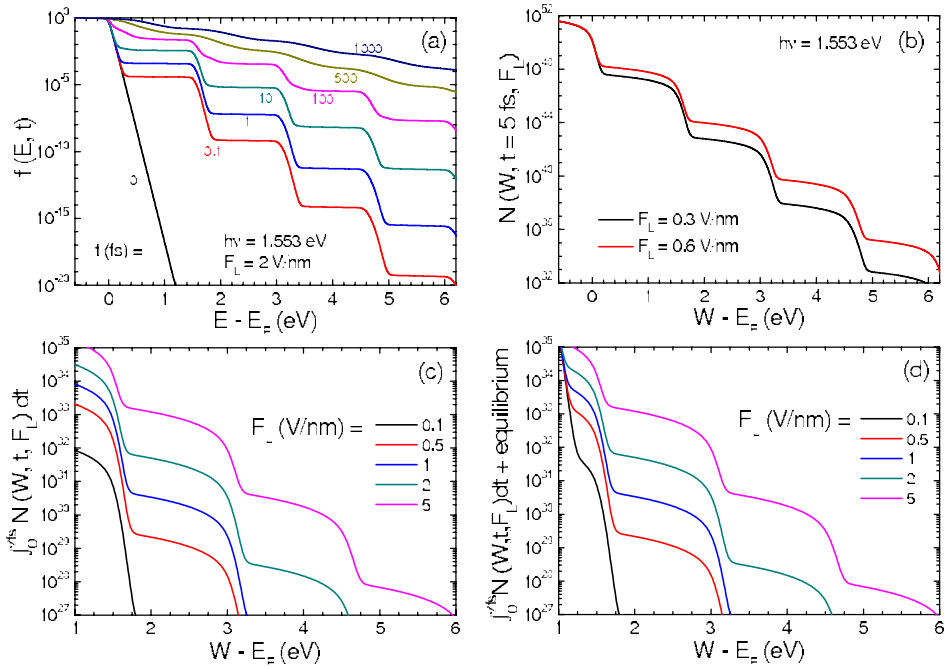

FIG. 1. (Color online) (a) Temporal evolution of electron energy distribution function $f(E,t)$ under a 1 ps laser (λ=800 nm or $h\nu$=1.553 eV) excitation at F_L=2 V/nm. (b) The instantaneous $N(W,t)$ (eV^{-1} m^{-2} s^{-1}) at t=5 fs for F_L =0.3 (bottom) and 0.6 V/nm (top). The time-integrated $N(W)$ (eV^{-1} m^{-2}) at different F_L from 0.1 (bottom) to 5 V/nm (top) for the calculation (c) within the laser-pulse duration of 7 fs and (d) including the long-time (100 s) equilibrium contribution.

C. Laser perturbation and energy absorption

Free electrons oscillating in the laser field can absorb photon energy only when mechanisms exist to conserve both energy and momentum. With laser light of frequency ω and amplitude of electric field F_L, the photon absorption (mediated by electron-phonon collisions) term reads

$$\left.\frac{\partial f(k)}{\partial t}\right|_{\text{absorb}} = \frac{2\pi}{\hbar}\sum_{\boldsymbol{q}}|M_{ep}|^2\sum_l J_l^2\left(\frac{e\boldsymbol{F}_L\cdot\boldsymbol{q}}{m_e\omega^2}\right)\{S^-(\boldsymbol{k},\boldsymbol{q}) \times \delta[E(k)-E(k^-)-E_{\text{ph}}(q)+l\hbar\omega]+S^+(\boldsymbol{k},\boldsymbol{q}) \times \delta[E(k)-E(k^+)+E_{\text{ph}}(q)+l\hbar\omega]\}, \quad (7)$$

where the perturbation occurs when an oscillating electron collides with a phonon absorbing or emitting its momentum. The probability of absorption (or emission) of l photons is given by the square of the Bessel function. The product $\boldsymbol{F}_L\cdot\boldsymbol{q}$ in the argument of the Bessel function indicates that the absorption of the photon is allowed only if the change in the electron wave vector $\boldsymbol{q}$ has a component parallel to the laser field $\boldsymbol{F}_L$. Since we do not consider a definite polarization of laser light, an average is made over all directions of the laser field.

To solve Eq. (1) numerically, the collision sums in Eqs. (2), (4), (5), and (7) are transformed analytically into collision integrals.[16] The system of nonlinear integrodifferential equations and the collision integrals can be rewritten depending on time and energy using the dispersion relation of electrons $E=\hbar^2k^2/2m_e$ and phonons $E_{\text{ph}}=\hbar v_s q$. By considering discrete E and E_{ph}, we have a system of fully coupled nonlinear ordinary equations. The integration over time is done by applying Euler's algorithm with adaptive time steps. With this procedure, for given values of laser wavelength (λ), laser frequency (ν) or angular frequency (ω), amplitude of laser field strength (F_L), and laser-pulse duration (τ), we are able to calculate the time evolution of the distribution functions of the electron gas $f(E,t)$ and the phonon gas $g(E_{\text{ph}},t)$. From the time-dependent electron energy distribution function, the emission of electrons or current density $J(t)$ can be obtained for a given material's work function ϕ (see Sec. III).

III. RESULTS

Consider a tungsten tip is subjected to a laser excitation (F_L=2 V/nm) of λ=800 nm with a pulse duration up to τ =1 ps. Figure 1(a) shows the temporal evolution of $f(E,t)$ versus electron energy with respect to the Fermi level E_F. Before the excitation at t=0, the tungsten is described by a Fermi-Dirac distribution function at 300 K. The laser excitation creates a strong nonequilibrium distribution, characterized by a steplike profile with an increase in $E-E_F$ equal to the photon energy $h\nu$=1.553 eV. For example, the first change is from E_F to $E_F+h\nu$, which is due to one-photon absorption process by electrons between $E_F-h\nu$ and E_F. Excited electrons can subsequently absorb a further photon, leading to an occupation number increase for electron energies up to $2h\nu$ above E_F and so on for $nh\nu$ above E_F. From the figure, the steplike characteristic is dominant until about 100 fs, and the smoothing effect (due to e-e and e-p collisions) will start to occur. At about 500 fs or more, the electron energy redistribution will modify $f(E)$ toward a new quasiequilibrium Fermi-Dirac distribution at a higher temperature. Thus the TTM is justified for picosecond laser excitation on metals but not for femtosecond laser pulse ($<$100 fs), where the steplike profile remains present at the end of laser perturbation. Note that the relaxation time is longer than the decaying time scaling of $1/(E-E_F)^2$ after an electron is excited to an energy state E above E_F because the secondary electrons are created in the excitation, and the exact time to reach the new thermalized state by many

electron-electron collisions will depend on laser power and duration.[16,17]

From the free-electron theory of metals, the number of electrons per unit area and time with total energy between E and $E+dE$ and normal energy (with respective to barrier surface) between W and $W+dW$ is $N(E,W,t)dEdW = \frac{m}{2\pi^2\hbar^3} f(E,t)dEdW$. For the electron emission from the ultrafast laser-excited metal surface with a dc-biased voltage, the emitted current density is calculated by

$$J(t) = e\int_0^\infty N(W,t)D(W)dW,$$

where

$$N(W,t)dW = \frac{mdW}{2\pi^2\hbar^3}\int_W^\infty f(E,t)dE. \quad (8)$$

Here $N(W,t)dW$ is the instantaneous number of electrons with normal energy between W and $W+dW$ impinging on the surface barrier per unit area and time, which is plotted in Fig. 1(b) at $t=5$ fs within a 7 fs laser pulse for $F_L=0.3$ and 0.6 V/nm. To compare with the time-average experimental measurement,[8] we first integrate the calculated $N(W,t)$ over the entire laser-pulse duration from 0 to 7 fs, which is shown in Fig. 1(c) at various $F_L=0.1-5$ V/nm. It is difficult to have a direct comparison as the time taken in the time-average data[8] is unknown to us; we consider that the measurement should consist of the contribution from the electron emission from the equilibrium state. In doing so, we add an equilibrium component of $N_{\text{eqm}}(W)\times T(T=100\text{ s})$, and the result is shown in Fig. 1(d). From the figure, we conclude that the equilibrium condition will only modify the low-energy component close to the Fermi energy, and the non-equilibrium or nonthermal component is at higher-energy level 2–6 eV, confirming qualitatively the experimental finding.[8]

With the supply function of electrons incident on the metal-vacuum interface shown in Fig. 1(b), depending on their respective normal energy W, these excited electrons (under nonequilibrium condition) will transmit through a surface barrier with finite probability $D(W)$, giving the instantaneous emitted current density $J(t)$. The electron-tunneling probability $D(W)$ is calculated through a simplified potential barrier of $V(x)=\phi-e^2/(16\pi\epsilon_0 x)-exF_{\text{dc}}$ using a modified Wentzel-Kramers-Brillouin (WKB) method.[20] In Fig. 2, the calculated results of $N(W)D(W)$ at various $F_{\text{dc}}=0.001-1$ V/nm are plotted as a function of $W-E_F$. It is clear that at small dc field F_{dc}, only electrons with $W>E_F+\phi$ are able to emit over the barrier as pure photoemission. At $F_{\text{dc}}=1$ V/nm, significant amount of electrons in the range of $W-E_F=0-6$ eV are emitted through both field and overbarrier emission.

The electron emission rate from femtosecond laser-excited metal surface under dc bias will depend on both the laser field F_L (or laser power P as $F_L\propto P^{1/2}$) and the dc field F_{dc} (or tip bias V_g as $F_{\text{dc}}\propto V_g$). It is assumed that the assigned arbitrary values of F_{dc} in our calculations have included the geometrical enhancement factor of dc field on the sharp tip. In Fig. 3(a), for a 10 fs laser ($h\nu=1.553$ eV) excitation on a tungsten tip ($\phi=4.4$ eV), the calculated J at $t=10$ fs are plotted in symbols as function of laser field F_L for three different dc electric fields F_{dc}, which can be fitted by a power law $J\propto(F_L)^{2n}$ (dashed lines), i.e., $J\propto P^n$, with $n=2.91$, 2.12, and 1.16, for $F_{\text{dc}}=0.001$, 1, and 3 V/nm. This finding indicates a reduced power dependence of J (or electron counts) on F_L (or P) for increased F_{dc} (or V_g), which have also been generally observed in recent experiments.[8,9] From our model, at small F_{dc}, it is the pure multiphoton electron emission,

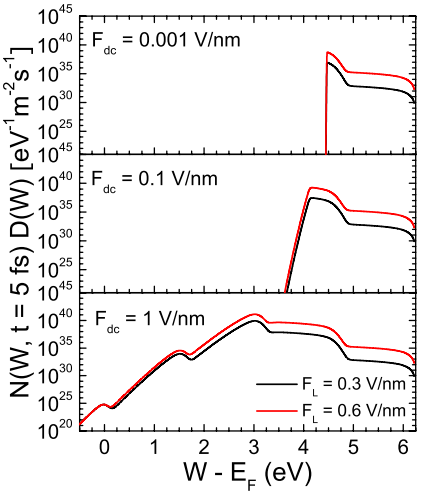

FIG. 2. (Color online) The energy spectrum of emitted electrons at the end of a 5 fs laser excitation on a tungsten tip with a work function of 4.4 eV for various applied dc field: $F_{\text{dc}}=0.001$, 0.1, and 1 V/nm, including two different laser excitation fields of $F_L=0.3$ (bottom) and 0.6 V/nm (top).

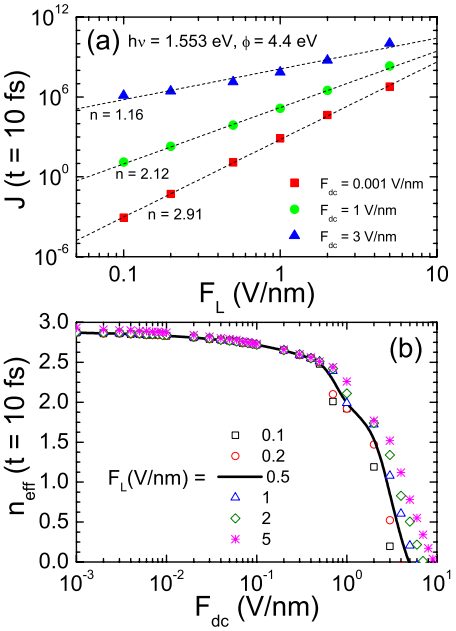

FIG. 3. (Color online) The dependence of (a) J and (b) n_{eff} on various F_L and F_{dc} for a 10 fs laser ($h\nu=1.553$ eV) excitation on a tungsten tip ($\phi=4.4$ eV). The dashed lines in (a) are fitted by a power law $y\propto x^{2n}$. The solid line in (b) is the baseline calculation at $F_L=0.5$ V/nm.

satisfying $nh\nu \geq \phi$. As F_{dc} increases, significant amount of electrons are emitted through tunneling process (field emission), which are responsible for small values of fitted n.

However from the experimental observations,[8,9] it is difficult to fit $J \propto (F_L)^{2n} \propto P^n$, with a constant n for large F_{dc} (>1 V/nm). This can also been seen from the relatively poor fitting of our calculations at large F_{dc} (=3 V/nm) as shown in Fig. 3(a). To solve this problem, we define an effective number of photon absorption as

$$n_{\text{eff}} = \frac{\bar{W} - E_F}{h\nu},$$

where

$$\bar{W}(t) = \frac{\int_0^\infty WN(W,t)D(W)dW}{\int_0^\infty N(W,t)D(W)dW}. \quad (9)$$

Here $\bar{W}(t)$ is the average emission energy. In Fig. 3(b), the calculated n_{eff} is plotted as a function of F_{dc} for various F_L =0.5 V/nm (solid line) and 0.1, 0.2, 1, 2, and 5 V/nm (symbols). It is observed that $n_{\text{eff}} \approx 2.87-2.93$ is approximately independent of F_L at small $F_{dc} < 0.1$ V/nm, which agrees well with the fitted $n=2.91$ at $F_{dc}=0.001$ V/nm as shown in Fig. 3(a). The discrepancy among the n_{eff} for different F_L is significant at large F_{dc}, which explains why fitting $J \propto (F_L)^{2n}$ is difficult at $F_{dc} > 1$ V/nm. For example, at F_{dc} =3 V/nm, the fitted n is 1.16 but the n_{eff} ranges from 0.2 to 1.5 depending on $F_L=0.1-5$ V/nm. The decrease in n_{eff} with smaller F_L could be understood by taking a closer look at Fig. 2 (the case $F_{dc}=1$ V/nm). The difference between $F_L=0.3$ (bottom) and 0.6 V/nm (top) increases with W, and the two cases overlap with each other for $W \leq E_F$. Therefore those excited electrons with $W > E_F$ will be more dominant in the emitted electron spectrum for 0.6 V/nm case, and the average emission energy and n_{eff} are both larger.

IV. COMPARISON TO EXPERIMENTS

It is not a trivial matter to experimentally measure the exact time evolution of ultrafast electron emission or duration in femtosecond or attosecond time scales. In order to have comparison with experimental time-integrated measurement, we first calculate the time-dependent $J(t)$ and perform the time integration over the laser-pulse duration.

A. Experiment I: Laser power dependence

In the two recent experimental measurements,[8,9] the electron flux has been studied as function of laser power P and tip bias V_g. It was found difficult to fit the electron counts $\propto (F_L)^{2n}$ or $\propto P^n$ with a constant n at large applied dc field $F_{dc} > 1$ V/nm. The difficulty lies in the significant amount of dc field emission current at large F_{dc}, where P^n scaling is only valid for pure multiphoton electron emission satisfying $nh\nu \geq \phi$. To solve this problem, we have defined an effective number of photon absorption n_{eff} as mentioned before. In Fig. 4, we compare the time-integrated n_{eff} (solid line) over the 50 fs laser-pulse duration to an experimental measurement of a 810 nm and 50 fs laser excitation on a metal surface with a work function of 6 eV.[9] Here, the range of F_{dc} from 0.25 to 1.25 V/nm corresponds to the dc applied voltage from 50 to 250 V based on the results reported in the paper.[9] The comparison shows a reasonable agreement with the experimental measurement (symbols). The calculations using TTM-based model (dashed lines) are also plotted at arbitrary temperatures of 1000, 2000, and 5000 K for comparison.

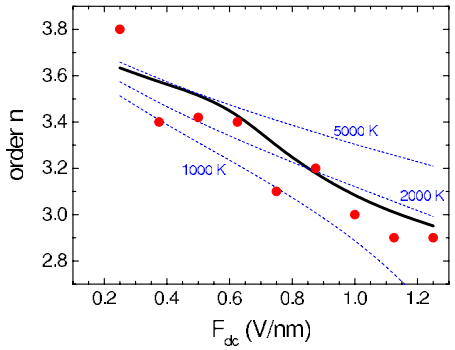

FIG. 4. (Color online) The comparison of the calculated time-integrated n based on the nonequilibrium model (solid line) at $h\nu$ =1.553 eV (800 nm) and $\phi=6$ eV with the measurement (symbols) (Ref. 9). The dashed lines are the calculations based on the equilibrium TTM at various temperatures.

B. Experiment II: Peak to baseline ratio

In another experiment,[7] the laser pulse is split into a pump and probe pulses, and a variable time delay between them can be provided. At zero delay, the two perfectly overlapping identical pulses will give the peak photocurrent, while the electron emission from the two pulses (at long-time delay) will become additive, giving the baseline photocurrent. To explain the experimental results, Hommelhoff *et al.*[7] included the process of optical-field emission by simply adding the optical electric field into the dc electric field term in the Fowler-Nordheim equation (assuming equilibrium electron distribution function),

$$\frac{I_{\text{peak}}}{I_{\text{base}}} = \frac{(2F_L + F_{dc})^2}{2(F_L + F_{dc})^2} \exp\left\{ B\phi^{3/2} \left[\frac{v(y_1)}{F_L + F_{dc}} - \frac{v(y_2)}{2F_L + F_{dc}} \right] \right\}, \quad (10)$$

where $B=6.8308$ eV$^{-3/2}$ V nm^{-1}, $v(y)$ are Nordheim parameters with $y_1 = 3.79 \times 10^{-5} \sqrt{F_L + F_{dc}}/\phi$ and $y_2 = 3.79 \times 10^{-5} \sqrt{2F_L + F_{dc}}/\phi$. It was reported that the best fit to their experimental results is with a laser field of about F_L =1.8 V/nm, which is about five times higher than the average laser field (0.3–0.4 V/nm) due to the local-field enhancement. By using their proposed quasistatic equilibrium model with optical-field emission at $F_L=1.8$ V/nm, the results based on Eq. (10) are plotted in Fig. 5(a) for various work function $\phi=2.1$, 2.4, and 3 eV. It is found that the best fit to experimental results (symbols) in Fig. 5(a) will require a

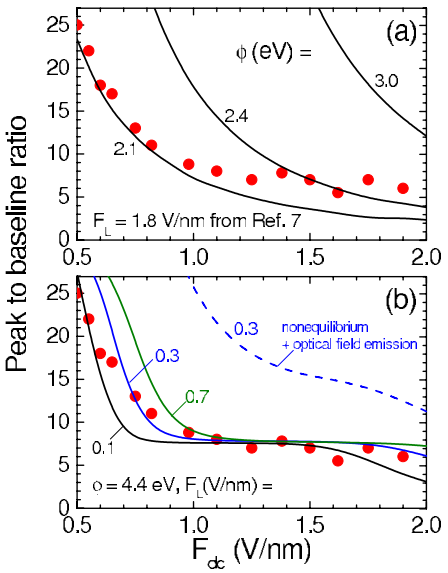

FIG. 5. (Color online) The calculated peak to baseline ratio of the emitted charge density from a tungsten tip excited by a 8 fs ultrafast laser with an optical field of F_L as a function of the applied dc field F_{dc}=0.5–2 V/nm. (a) The calculations based on the reported quasistatic equilibrium model (Ref. 7) (including optical-field emission) at F_L=1.8 V/nm for various work function ϕ=2.1, 2.4, and 3 eV. (b) The calculations based on our proposed nonequilibrium laser excitation model without optical-field emission at a realistic work function of ϕ=4.4 eV for F_L=0.1, 0.3, and 0.7 V/nm (without optical-field enhancement). The dashed line in (b) is to show the comparison if optical-field emission is added into the nonequilibrium model at F_L=0.3 V/nm. The symbols in (a) and (b) are the reported measurements (Ref. 7).

work function of about ϕ=2.1 eV, which is inconsistent for a tungsten tip. If a more realistic ϕ=4.5 eV (not shown) is used with the same F_L=1.8 V/nm, their proposed model based on Eq. (10) gives a much higher value of 282 207–192 (as compared to experimental results of about 25–5) in the range of F_{dc}=0.5–2 V/nm. Note if we use a better approximation from a recent paper[21] in calculating the function of $v(y)$, the revised calculated ratio is about 460 780–295.

On the other hand, without including the optical-field emission, our nonequilibrium model is able to give reasonable good agreement (solid lines) with a realistic work function of ϕ=4.4 eV as shown in Fig. 5(b) by using the laser average optical field of F_L=0.1–0.7 V/nm, with a best fit at about F_L=0.3 V/nm. Note it is consistent to use the average laser field without including the field enhancement of the optical field, as our model only considers the laser excitation on a bulk metal surface, without including the local excitation (see discussion below). In our calculations, the peak to baseline ratio is simply determined by taking the time average of the current density $J(t)$ as $[\int J(2F_L)dt]/[2\int J(F_L)dt]$, where the peak value has twice the amount of laser excitation as compared to the baseline excitation. If we arbitrarily include the optical-field emission into our calculations (based on the nonequilibrium carrier distribution) by simply adding the F_L into the F_{dc} term, the calculations will have poor agreement. For example, a comparison (dashed line) at F_L =0.3 V/nm is plotted in Fig. 5(b). Thus, our nonequilibrium model can explain the prior experimental results[7] without using the disputed optical-field emission, which had not been reported in many other experiments.

V. REMARKS

From our calculated results and verifications with experimental results, it is clear that the nonequilibrium model proposed in this paper is able to explain the experimental findings within the operating parameters.[7–9] We have suggested the possible errors in the analysis of using a quasistatic optical-field emission model to explain the experiment results,[7] while a single-energy time-dependent Schrödinger model has also been claimed by the same paper[7] to prove the optical-field emission without any adjustable parameters. This justification is however misleading for the following reasons. First, the model has assumed a ground-state wave function (−13.5 eV), which is not justified as the electrons emitted from the surface should have an energy level near Fermi energy of −4.5 eV. Instead of using the same optical field of 1.8 V/nm (as done in the quasistatic model), the time-dependent model used a different optical field of 2.7 V/nm to obtain good agreement (see Figs. 2 and 3 in Ref. 7). For any tunneling problem across a time-dependent barrier, it is known that the tunneling particles (such as electrons) interacting with the modulating field will emit or absorb the modulation quanta $\hbar\omega$ (which is about 1.553 eV at 800 nm). Thus simply solving the single-energy Schrödinger equation[7] will not be able to resolve this issue. Finally, if we compare the two models proposed by the paper,[7] we see that the erroneous quasistatic model actually has a better agreement than the claimed consistent time-dependent model (see Fig. 2 in Ref. 7). It is reasonable to question the validity of the proposed optical-field emission mechanism, which has not been observed in many other experiments.[8,9,22,23] It may be argued that optical-field emission will require a higher laser power or to operate at a much smaller dc applied electric field. However, two recent experiments[22,23] did not observe optical-field emission from their respective measured laser-induced electron emission from sharp Mo tips and metallic nanoparticles, which operate at high laser power[22] or low dc field.[23] A simple way to compare the importance between the optical-field emission and laser-excited photofield emission is to measure the energy distribution of the emitted electron as done before.[8] If optical-field emission is more important, we will not observe the calculated steplike distribution as shown in Fig. 1(d).

Here, we would like to comment on the limitations of our model for further improvements. Our model is based on a bulk metal surface without considering the local laser excitation process on a sharp tip, which might be improved by modifying the localized electronic structures. If such effects are included, we expect the separation between the quantized energy level will increase with small size. This will lead to a reduced coupling between the electron and phonon subsystems, which will remain in the nonequilibrium state much longer. Thus, we speculate that the proposed nonequilibrium carrier distribution will become more dominant for laser ex-

citation on nanometer scale, which was also supported by a recent experiment[23] in using ultrafast laser to excite electron emission from metallic nanoparticles of different sizes. The good agreement of our bulk laser excitation model can be seen as an analogy to the well-known Fowler-Nordheim law in explaining dc field emission from a sharp nanotip even if it is also based on the bulk electronic structure. However, revision may be needed when the size of the tip is approaching single atom limit.[24]

The second limitation is that we have used a semiclassical approach (Boltzmann's equation) in the studies of the laser excitation on metallic surface, where many-body quantum effects are ignored. Such semiclassical treatment may be valid for metals, but a more consistent treatment based on nonequilibrium Green's-function theory[19] should be used especially for a semiconductor. Note wide band-gap semiconductor such as GaAs will be of interest for ultrafast laser-induced electron emission as GaAs has a higher quantum efficiency as compared to metal. The effects of the electron's space-charge field[25] and finite tunneling time[26] have also ignored in our model. Finally, to develop a comprehensive model to combine the nonequilibrium laser excitation and consistent time-dependent tunneling process including optical tunneling from a sharp tip is not a trivial matter, which is beyond the scope of this paper. Further verification of the time-dependent electron pulse can be done by using ultrafast time-resolved measurement.[27]

VI. CONCLUSIONS

To summarize, a nonequilibrium model based on Boltzmann's equation has been used to explain the electron emission process from a dc-biased metallic surface under the excitation of a low-power femtosecond laser pulse conducted in recent experiments.[6–9] Our model is able to confirm the gradual decrease in the power dependence from a high-order nonlinearity at low bias to linear order emission at high bias voltages observed in the experiments. Good agreements with the experimental measurements[7,9] has been obtained. The calculations shown in this paper and the majority of experimental results seem to suggest that laser excitation electron emission may be more important than the optical-field emission within the reported operating parameters.

ACKNOWLEDGMENTS

This work was supported by a Singapore A*STAR grant (Grant No. 042 101 0080), NTU RGM 5/05 grant, and a AFOSR AOARD grant.

*Author to whom correspondence should be addressed; elkang@ntu.edu.sg

[1] A. H. Zewail, Annu. Rev. Phys. Chem. **57**, 65 (2006).
[2] H. Ihee, V. A. Lobastov, U. M. Gomez, B. M. Goodson, R. Srinivasan, C. Y. Ruan, and A. H. Zewail, Science **291**, 458 (2001).
[3] H. Niikura, F. Legare, R. Hasbani, A. D. Bandrauk, M. Y. Ivanov, D. M. Villeneuve, and P. B. Corkum, Nature (London) **417**, 917 (2002).
[4] B. J. Siwick, J. R. Dwyer, R. E. Jordan, and R. J. D. Miller, Science **302**, 1382 (2003).
[5] M. Merano, S. Sonderegger, A. Crottini, S. Collin, P. Renucci, E. Pelucchi, A. Malko, M. H. Baier, E. Kapon, B. Deveaud, and J.-D. Ganiere, Nature (London) **438**, 479 (2005).
[6] P. Hommelhoff, Y. Sortais, A. Aghajani-Talesh, and M. A. Kasevich, Phys. Rev. Lett. **96**, 077401 (2006).
[7] P. Hommelhoff, C. Kealhofer, and M. A. Kasevich, Phys. Rev. Lett. **97**, 247402 (2006).
[8] C. Ropers, D. R. Solli, C. P. Schulz, C. Lienau, and T. Elsaesser, Phys. Rev. Lett. **98**, 043907 (2007).
[9] B. Barwick, C. Corder, J. Strohaber, N. Chandler-Smith, C. Uiterwaal, and H. Batelaan, New J. Phys. **9**, 142 (2007).
[10] R. Ganter, R. Bakker, C. Gough, S. C. Leemann, M. Paraliev, M. Pedrozzi, F. Le Pimpec, V. Schlott, L. Rivkin, and A. Wrulich, Phys. Rev. Lett. **100**, 064801 (2008).
[11] C. Hernandez-Garcia, M. L. Stutzman, and P. G. O'Shea, Phys. Today **61**(2), 44 (2008).
[12] J. W. G. Tisch, Nat. Phys. **4**, 350 (2008).
[13] J. P. Marangos, Nature (London) **446**, 619 (2007).
[14] G. L. Yudin and M. Y. Ivanov, Phys. Rev. A **64**, 013409 (2001).
[15] L. V. Keldysh, Zh. Eksp. Teor. Fiz. **47**, 1945 (1964) [Sov. Phys. JETP **20**, 1307 (1965)].
[16] B. Rethfeld, A. Kaiser, M. Vicanek, and G. Simon, Phys. Rev. B **65**, 214303 (2002).
[17] L. D. Pietanza, G. Colonna, S. Longo, and M. Capitelli, Eur. Phys. J. D **45**, 369 (2007).
[18] K. L. Jensen, N. A. Moody, D. W. Feldman, E. J. Montgomery, and P. G. O'Shea, J. Appl. Phys. **102**, 074902 (2007).
[19] H. Haug and A.-P. Jauho, *Quantum Kinetics in Transport and Optics of Semiconductors* (Springer, New York, 1996).
[20] K. L. Jensen and M. Cahay, Appl. Phys. Lett. **88**, 154105 (2006).
[21] R. G. Forbes, Appl. Phys. Lett. **89**, 113122 (2006).
[22] S. Tsujino, P. Beaud, E. Kirk, T. Vogel, H. Sehr, J. Gobrecht, and A. Wrulich, Appl. Phys. Lett. **92**, 193501 (2008).
[23] A. Gloskovskii, D. A. Valdaitsev, M. Cinchetti, S. A. Nepijko, J. Lange, M. Aeschlimann, M. Bauer, M. Klimenkov, L. V. Viduta, P. M. Tomchuk, and G. Schonhense, Phys. Rev. B **77**, 195427 (2008).
[24] Y. Gohda and S. Watanabe, Phys. Rev. Lett. **87**, 177601 (2001).
[25] L. K. Ang and P. Zhang, Phys. Rev. Lett. **98**, 164802 (2007).
[26] M. Buttiker and R. Landauer, Phys. Rev. Lett. **49**, 1739 (1982).
[27] P. Reckenthaeler, M. Centurion, V. S. Yakovlev, M. Lezius, F. Krausz, and E. E. Fill, Phys. Rev. A **77**, 042902 (2008).